

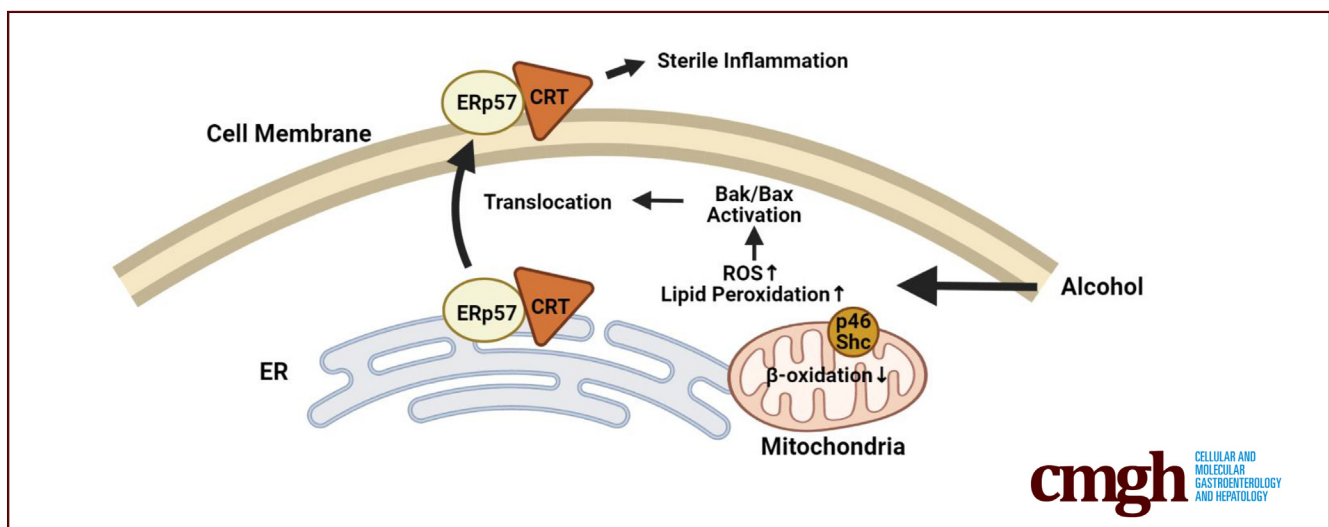
## ORIGINAL RESEARCH

## Shc Is Implicated in Calreticulin-Mediated Sterile Inflammation in Alcoholic Hepatitis



Yuan Li,<sup>1</sup> Joy X. Jiang,<sup>2</sup> Weiguo Fan,<sup>1</sup> Sarah R. Fish,<sup>2</sup> Suvarthi Das,<sup>1</sup> Parul Gupta,<sup>1</sup> Gergely Mozes,<sup>1</sup> Lorand Vancza,<sup>1</sup> Sutapa Sarkar,<sup>1</sup> Koshi Kunimoto,<sup>1</sup> Dongning Chen,<sup>1</sup> Hyesuk Park,<sup>1</sup> Dahn Clemens,<sup>3</sup> Alexey Tomilov,<sup>4</sup> Gino Cortopassi,<sup>4</sup> and Natalie J. Török<sup>1</sup>

<sup>1</sup>Gastroenterology and Hepatology, Stanford University, VA Palo Alto, Palo Alto, California; <sup>2</sup>Gastroenterology and Hepatology, University of California Davis Medical Center, Sacramento, California; <sup>3</sup>Internal Medicine, University of Nebraska Medical Center, Omaha, Nebraska; and <sup>4</sup>Molecular Biosciences, School of Veterinary Medicine, University of California Davis, Davis, California



## SUMMARY

We describe the role of Src homology and collagen proteins in alcoholic steatohepatitis. p46 Src homology and collagen mediates lipid peroxidation, oxidative stress, and calreticulin translocation to the membrane, where it acts as a damage-associated molecular pattern. Src homology and collagen inhibition reduces inflammation in alcoholic liver injury.

**BACKGROUND & AIMS:** Src homology and collagen (Shc) proteins are major adapters to extracellular signals, however, the regulatory role of Shc isoforms in sterile inflammatory responses in alcoholic hepatitis (AH) has not been fully investigated. We hypothesized that in an isoform-specific manner Shc modulates pre-apoptotic signals, calreticulin (CRT) membrane exposure, and recruitment of inflammatory cells.

**METHODS:** Liver biopsy samples from patients with AH vs healthy subjects were studied for Shc expression using DNA microarray data and immunohistochemistry. Shc knockdown (hypomorph) and age-matched wild-type mice were pair-fed according to the chronic-plus-binge alcohol diet. To analyze

hepatocyte-specific effects, adeno-associated virus 8-thyroxine binding globulin-Cre (hepatocyte-specific Shc knockout)-mediated deletion was performed in *flox/flox* Shc mice. Lipid peroxidation, proinflammatory signals, redox radicals, reduced nicotinamide adenine dinucleotide/oxidized nicotinamide adenine dinucleotide ratio, as well as cleaved caspase 8, B-cell-receptor-associated protein 31 (BAP31), Bcl-2-associated X protein (Bax), and Bcl-2 homologous antagonist killer (Bak), were assessed in vivo. CRT translocation was studied in ethanol-exposed p46Shc $\delta$ SH2-transfected hepatocytes by membrane biotinylation in conjunction with phosphorylated-eukaryotic initiation factor 2 alpha, BAP31, caspase 8, and Bax/Bak. The effects of idebenone, a novel Shc inhibitor, was studied in alcohol/pair-fed mice.

**RESULTS:** Shc was significantly induced in patients with AH ( $P < .01$ ). Alanine aminotransferase, reduced nicotinamide adenine dinucleotide/oxidized nicotinamide adenine dinucleotide ratios, production of redox radicals, and lipid peroxidation improved ( $P < .05$ ), and interleukin  $1\beta$ , monocyte chemoattractant protein 1, and C-X-C chemokine ligand 10 were reduced in Shc knockdown and hepatocyte-specific Shc knockout mice. In vivo, Shc-dependent induction, and, in hepatocytes, a p46Shc-dependent increase in pre-apoptotic proteins Bax/Bak, caspase 8, BAP31 cleavage, and membrane translocation of CRT/endoplasmic

reticulum-resident protein 57 were seen. Idenone protected against alcohol-mediated liver injury.

**CONCLUSIONS:** Alcohol induces p46Shc-dependent activation of pre-apoptotic pathways and translocation of CRT to the membrane, where it acts as a damage-associated molecular pattern, instigating immunogenicity. Shc inhibition could be a novel treatment strategy in AH. (*Cell Mol Gastroenterol Hepatol* 2023;15:197–211; <https://doi.org/10.1016/j.jcmgh.2022.09.005>)

**Keywords:** Alcoholic Hepatitis; Shc; Calreticulin; Lipid Peroxidation; Sterile Inflammation.

**A**lcoholic hepatitis (AH) is a severe form of alcoholic liver disease that carries high mortality. Clinically, it is characterized by severe inflammation, a rapid decline in liver synthetic function, and, often, death. The pathogenesis of AH has distinct features with lipid peroxidation, severe redox stress, sterile inflammation, and monocytic and neutrophil recruitment. As to how these processes are interlinked, however, has not been well understood.

The group of Src homology and collagen (Shc) proteins are important adapters to extracellular signals, and are involved in aging-related pathways,<sup>1</sup> regulate receptor tyrosine kinase,<sup>2</sup> and insulin signaling.<sup>3</sup> Shc proteins derive from the ShcA locus: p46 and p52Shc are generated from different start codons, whereas p66Shc is a product of alternative splicing. The p66Shc isoform has been studied in alcohol-induced liver injury in vitro and in animal experiments.<sup>4,5</sup> However, the mouse models used were not always clear p66Shc knockouts (KOs), and the other isoforms were reduced as well (hypomorphs). In addition, the other mitochondrial isoform, p46Shc, shows more substantial induction upon alcohol treatment, therefore further studies are needed to delineate its role in the context of alcoholic hepatitis. Calreticulin (CRT), an endoplasmic reticulum (ER)-resident protein that is involved in Ca<sup>2+</sup> signaling, upon danger signals exits the ER, and translocates to the membrane to act as a damage associated molecular pattern (DAMP) molecule signaling for recognition by immune cells.<sup>6,7</sup> The role of CRT as a DAMP in AH is unclear, and, given the redox-sensitive adapter role of Shc, we postulated that Shc-mediated oxidative signals and lipid peroxidation may lead to the activation of pre-apoptotic pathways in response to alcohol, prompting CRT translocation.<sup>8,9</sup>

In this study, our goal was to decipher how Shc-mediated CTR membrane translocation is involved in generating pre-apoptotic and proinflammatory signals in alcoholic hepatitis, and whether Shc inhibition could represent a novel therapeutic approach.

## Results

### Shc Is Induced in Patients With AH

To study Shc in age-matched AH patients, first we analyzed DNA microarrays.<sup>10</sup> SHC1 gene expression was induced in the livers of AH patients compared with livers from healthy subjects (Figure 1A). Immunohistochemistry (IHC) on liver biopsy samples from patients with AH


showed increased Shc signal mainly in hepatocytes, in contrast to healthy controls (Figure 1B). Consistently, the liver *Shc* messenger RNA transcripts were associated positively with serum alanine aminotransferase (ALT) levels in our mouse model of alcoholic liver injury, which is discussed further later (Figure 1C).

### Shc Knockdown and Hepatocyte-Specific Shc Knockout Mice Are Protected Against Alcohol-Induced Liver Injury and Oxidative Stress

To study the role of Shc in AH, we first evaluated Shc knockdown (hypomorph, Shc<sup>KD</sup>) mice that show a decrease in all Shc isoforms (hypomorphs; total Shc deletion is embryonically lethal). Mice were pair-fed a chronic-plus-binge alcohol diet (National Institute on Alcohol Abuse and Alcoholism [NIAAA] protocol).<sup>11</sup> p66Shc was very low at baseline and did not show induction after the NIAAA diet (Figure 2A). Shc<sup>KD</sup> mice had significantly lower serum ALT levels compared with wild-type (WT) mice on the NIAAA diet (Figure 2B). Alcohol is known to be oxidized by alcohol dehydrogenase and acetaldehyde dehydrogenase and increase the reduced nicotinamide adenine dinucleotide (NADH)/oxidized nicotinamide adenine dinucleotide (NAD<sup>+</sup>) ratio in the cytosol and mitochondria of hepatocytes,<sup>12</sup> and this was seen in our study. In alcohol-fed Shc<sup>KD</sup> mice, however, the NADH/NAD<sup>+</sup> ratio significantly decreased (Figure 2C). Lipid peroxidation as studied by 4-hydroxynonenal showed lower signal in Shc<sup>KD</sup> mice (Figure 2D).

We localized Shc predominantly to hepatocytes and confirmed that liver NADH/NAD<sup>+</sup> ratios were affected by Shc knockdown, and next we studied the role of hepatocyte Shc in alcoholic liver injury. Shc flox/flox (Shc<sup>f/f</sup>) mice were injected with either adeno-associated virus 8 (AAV8)-Cre on day 5 of the 10-day diet to delete Shc in hepatocytes, or by AAV8-control virus as control (Figure 3A). Hepatocyte-specific Shc knockout (Shc<sup>HepKO</sup>) (mice injected with AAV8-Cre) mice had improved histology, lower lipid peroxidation (4-hydroxynonenal signal) (Figure 3B), and significantly lower serum ALT levels (Figure 3C) compared with mice injected

**Abbreviations used in this paper:** AAV, adeno-associated virus; ACAA2, 3-ketoacyl CoA thiolase; AH, alcoholic hepatitis; ALT, alanine aminotransferase; Bak, Bcl-2 homologous antagonist killer; BAP31, B-cell receptor-associated protein 31; Bax, Bcl-2-associated X protein; CRT, calreticulin; CXCL10, C-X-C chemokine ligand 10; DAMP, damage-associated molecular pattern; ER, endoplasmic reticulum; ERp57, endoplasmic reticulum-resident protein 57; fl/fl, flox/flox; IHC, immunohistochemistry; IL1 $\beta$ , interleukin 1 $\beta$ ; KO, knockout; MCP-1, monocyte chemoattractant protein 1; NAD<sup>+</sup>, oxidized nicotinamide adenine dinucleotide; NADH, reduced nicotinamide adenine dinucleotide; NIAAA, National Institute on Alcohol Abuse and Alcoholism; PBS, phosphate-buffered saline; qPCR, quantitative polymerase chain reaction; ROS, reactive oxygen species; SDS, sodium dodecyl sulfate; Shc, Src homology and collagen; Shc<sup>HepKO</sup>, hepatocyte-specific Shc knockout; Shc<sup>KD</sup>, Shc knockdown/Shc hypomorph; SH2, Src homology 2 binding domain; siRNA, small interfering RNA; TG, triglyceride; WT, wild-type.

 Most current article

© 2022 The Authors. Published by Elsevier Inc. on behalf of the AGA Institute. This is an open access article under the CC BY-NC-ND license (<http://creativecommons.org/licenses/by-nc-nd/4.0/>).

2352-345X

<https://doi.org/10.1016/j.jcmgh.2022.09.005>

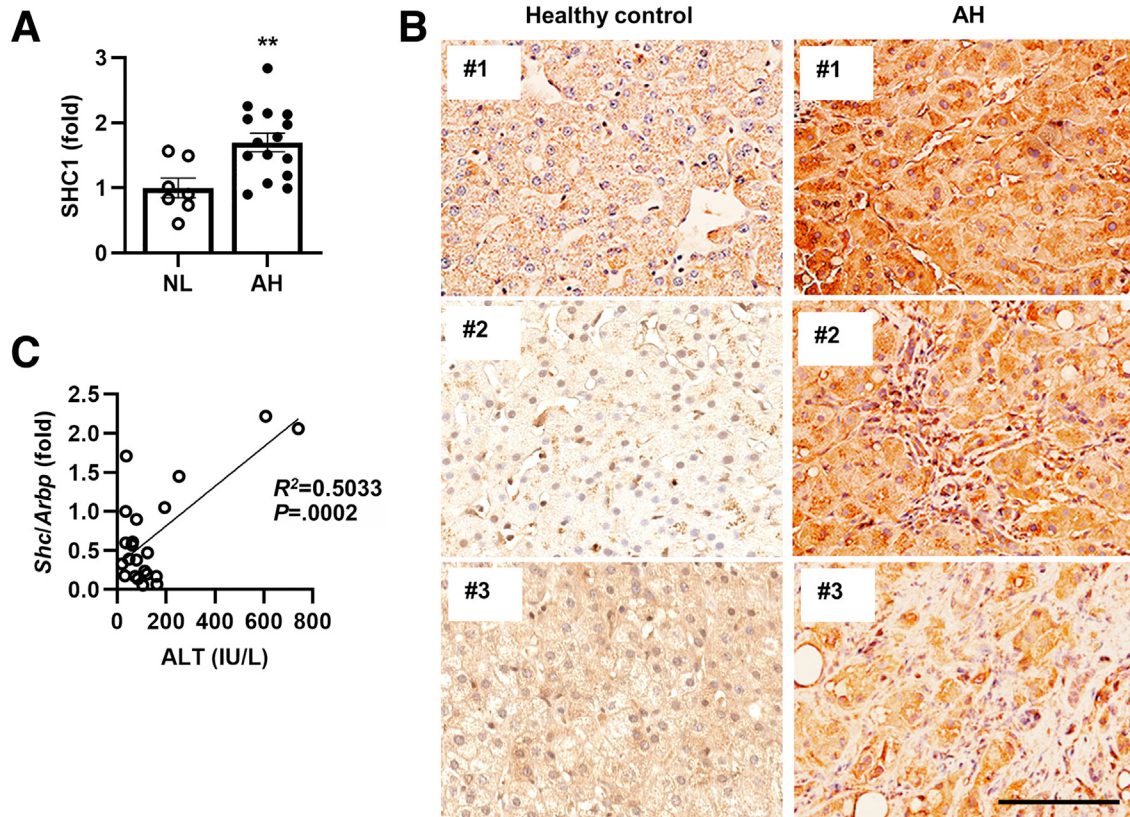


**Figure 1. Shc is induced in patients with AH.** (A) DNA array studies from 7 healthy subjects (normal liver [NL]) and 15 patients with severe AH showed significant induction of Shc in AH (means  $\pm$  SEM,  $**P < .01$ , database: GSE28619, <https://www.ncbi.nlm.nih.gov/geo/query/acc.cgi?acc=GSE28619>). (B) Immunohistochemistry for Shc was performed on biopsy samples from 3 healthy normal livers and 3 AH patients. Scale bar: 100  $\mu$ m. (C) The correlation coefficient of serum ALT levels and liver Shc messenger RNA levels (normalized to *Arbp*) was calculated (simple linear regression analysis,  $R^2 = 0.5033$ ;  $P < .001$ ).

with the control virus. In addition, the NIAAA diet induced production of reactive oxygen species (ROS) (Figure 3D) and NADH/NAD<sup>+</sup> ratios (Figure 3E), and these were significantly lower in *Shc<sup>HepKO</sup>* mice. Liver triglyceride (TG) assay and Oil red O staining indicated that liver steatosis mildly improved in *Shc<sup>HepKO</sup>* mice (Figure 3F and G).

### *Shc<sup>KD</sup>* and *Shc<sup>HepKO</sup>* Mice Show Lower Levels of Inflammatory Mediators

IHC showed a lower number of F4/80-positive monocytic cells in *Shc<sup>HepKO</sup>* mice on the NIAAA diet (Figure 4A). Reverse-transcription quantitative polymerase chain reaction (qPCR) showed that monocyte chemoattractant protein 1 (MCP-1), C-X-C chemokine ligand 10 (CXCL10), and interleukin 1 $\beta$  (IL1 $\beta$ ) were blunted in *Shc<sup>KD</sup>* (Figure 4B) and in *Shc<sup>HepKO</sup>* mice (Figure 4C). Luminex multiplex assay (Thermo Fisher Scientific) showed a reduction in MCP-1, IL-4, CXCL-10, and macrophage colony-stimulating factor in *Shc<sup>HepKO</sup>* mice (Figure 4D).

### Alcohol Induces Pre-apoptotic Changes and Calreticulin Translocation in a *Shc*-Dependent Pathway

Plasma membrane exposure of the ER-resident chaperone CRT as a DAMP has been linked to immunogenic cell

death.<sup>13</sup> Sterile inflammation is an important early pathogenic feature of AH, therefore it was tempting to speculate that CRT could be involved in mediating pre-apoptotic signals contributing to immunogenicity.

Alcohol is well recognized to activate different branches of the ER stress response.<sup>14,15</sup> CRT translocation as an early event can be mediated by ER stress signals, leading to an induction of pre-apoptotic pathways with caspase 8-dependent cleavage of B-cell-receptor-associated protein 31 (BAP31), and activation of Bcl-2-associated X protein (Bax) and Bcl-2 homologous antagonist killer (Bak).<sup>16,17</sup> Indeed, cleaved caspase-8 (p41/43, p18), BAP31 (p20), and Bax and Bak were seen in control virus-injected mice on the NIAAA diet, whereas these were attenuated in *Shc<sup>HepKO</sup>* mice (Figure 5A). To better capture CRT translocation, primary hepatocytes from WT and *Shc<sup>KD</sup>* mice were treated with ethanol. The signal in alcohol-treated hepatocytes showed a membrane pattern, however, this was much lower in *Shc<sup>KD</sup>* hepatocytes (Figure 5B). To further study CRT translocation in human cells we used HepG2 cells that express cytochrome p450 2E1 and alcohol dehydrogenase (VL-17A) cells.<sup>18</sup> Ethanol treatment resulted in CRT translocation to the cell surface (Figure 5C). Endoplasmic reticulum-resident protein 57 (ERp57) is a stress-responsive protein in the disulfide isomerase family that mainly resides in ER. CRT/ERp57 co-translocation to the



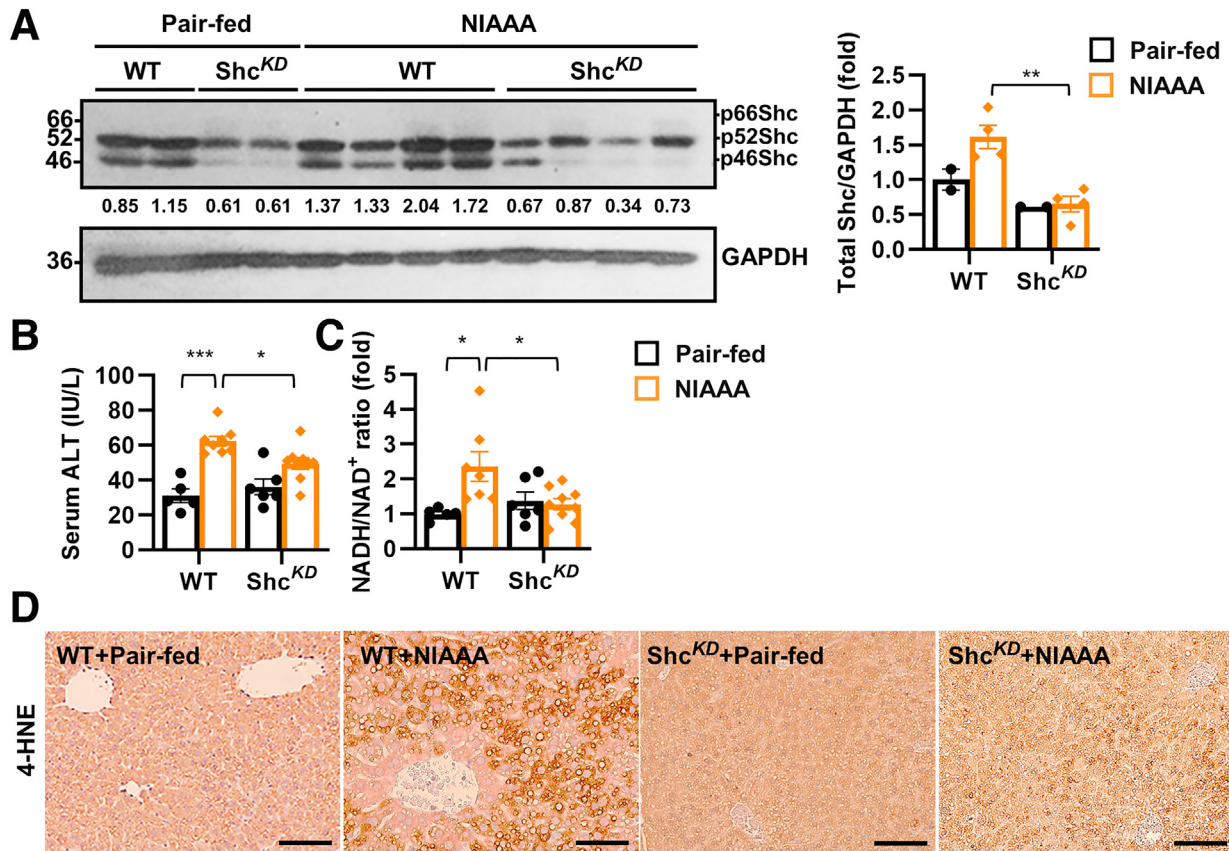


**Figure 2.** *Shc*<sup>KD</sup> in vivo improves lipid peroxidation, redox injury, ALT level, and NADH/NAD<sup>+</sup> ratios. WT and *Shc*<sup>KD</sup> mice were pair-fed the NIAAA diet. (A) Western blot analyses depicted that mainly the p52Shc and p46Shc isoforms were induced by the NIAAA diet, and in *Shc*<sup>KD</sup> mice these were attenuated (densitometry data presented as means  $\pm$  SEM, \*\**P* < .01). (B) Serum ALT levels and (C) liver NADH/NAD<sup>+</sup> ratios were increased significantly in WT mice on the NIAAA diet, but not in *Shc*<sup>KD</sup> mice. *n* = 5–9 mice per group. (D) 4-hydroxynonenal (4-HNE) immunohistochemistry showed decreased signal in *Shc*<sup>KD</sup> mice compared with WT mice after alcohol feeding. Scale bar: 100  $\mu$ m. All data are presented as means  $\pm$  SEM. \**P* < .05, \*\**P* < .01, and \*\*\**P* < .001. GAPDH, glyceraldehyde-3-phosphate dehydrogenase.

cell membrane signifies immunogenicity of cell death,<sup>19</sup> therefore we studied their surface presence in VL-17A cells after ethanol exposure. We isolated cell surface proteins by biotinylation, and found that both CRT and ERp57 increased after 16 hours of ethanol treatment (biotinylated), while the total protein level (input) remained similar over time (Figure 5D).

### The P46Shc Isoform Is Involved in Modulating Pre-apoptotic Signals After Alcohol Exposure

Shc proteins are known to modulate mitochondrial redox signaling, and the p66Shc isoform has been studied; however, in the liver its expression was low in basal or alcohol-fed conditions. Therefore, we focused on the role of the mitochondrial p46Shc isoform that was induced by the NIAAA diet. The Src homology 2 binding domain (SH2) has been described as essential to p46Shc binding and dysregulating 3-ketoacyl-CoA thiolase (ACAA2) activity, thereby inhibiting mitochondrial  $\beta$ -oxidation of fatty acids.<sup>20</sup> Indeed, markedly reduced ACAA2 activity was observed in alcohol-exposed rat livers.<sup>21</sup> Therefore, we transfected primary hepatocytes with p46Shc $\delta$ SH2 (Figure 6A) or control

plasmid, and exposed cells to alcohol. In p46Shc $\delta$ SH2-transfected, alcohol-exposed cells, most of the CRT signal remained perinuclear compared with mock-transfected alcohol-exposed cells in which we observed cell membrane exposure, as before (Figure 6B). CRT translocation can be mediated by ER stress response involving phosphorylation of the eukaryotic translation initiation factor 2 subunit  $\alpha$  and also specific pre-apoptotic events with caspase-8-activation.<sup>16,17</sup> In the mock-transfected alcohol-exposed cells, eukaryotic translation initiation factor 2 subunit  $\alpha$  was induced and activated, and we observed cleavage of caspase 8 and BAP31, as well as Bax and Bak induction. These effects of ethanol treatment were attenuated in p46Shc $\delta$ SH2-transfected cells (Figure 6C). In addition, alcohol-induced CRT translocation was blunted in VL-17A cells transfected with BAX siRNA (siBAX) (Figure 6D and E).

### Shc Inhibition Protects Against Alcohol-Induced Liver Injury In Vivo

Because p46Shc-specific inhibitors are not available, next we evaluated the efficacy of pharmaceutical Shc

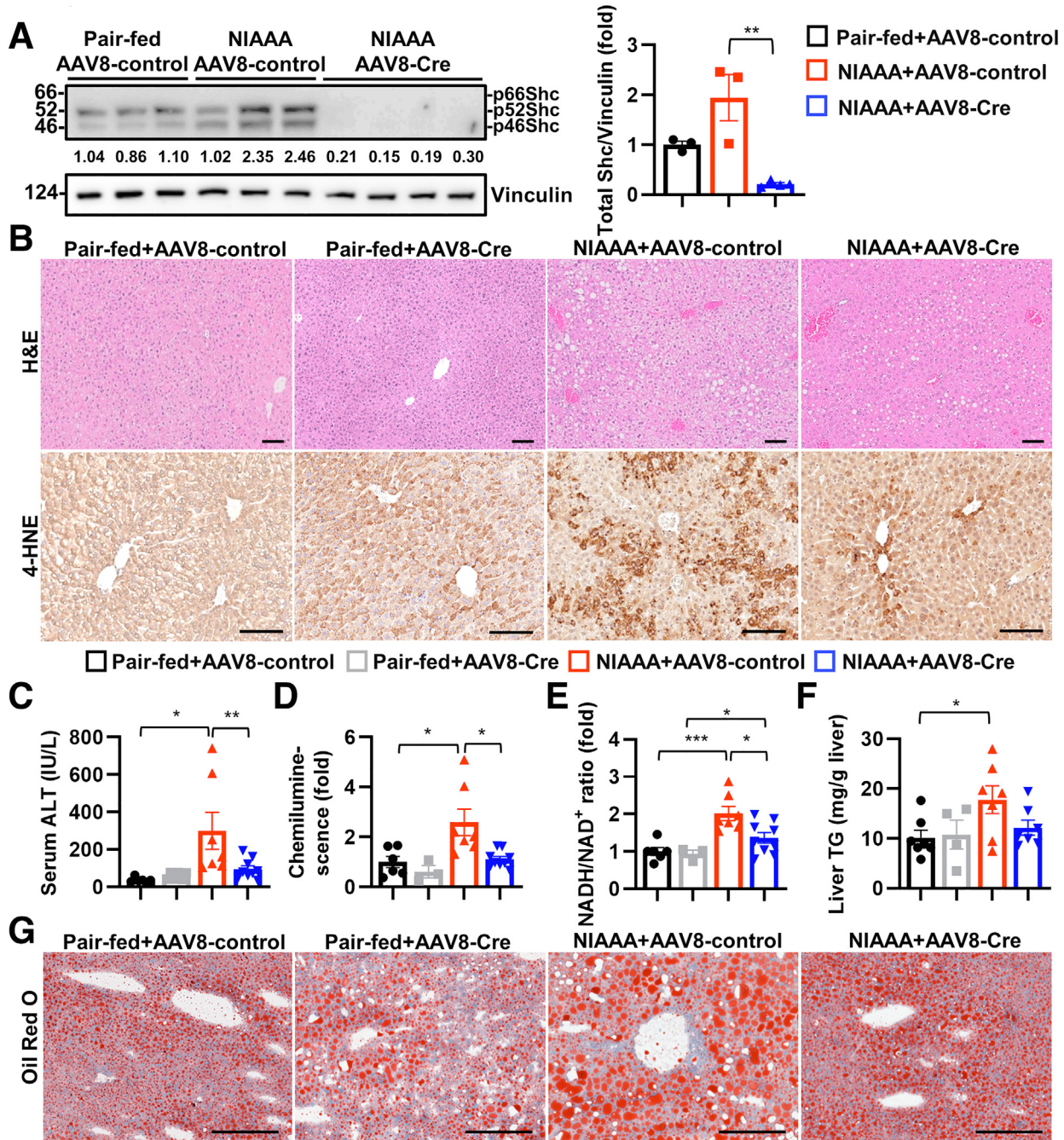


**Figure 3. AAV8-cre-mediated deletion of Shc from hepatocytes (*Shc<sup>HepKO</sup>*) in vivo improves lipid peroxidation, redox injury, decreases ALT levels, and NADH/NAD<sup>+</sup> ratios.** To study hepatocyte Shc, *Shc<sup>fl/fl</sup>* mice were placed on the NIAAA/pair-fed diet. On day 5 of the 10-day diet they were injected with either AAV8-Cre or AAV8 control ( $5 \times 10^{11}$  genome copies each). (A) Western blot shows Shc expression in the different models, densitometry depicts total Shc. (B) H&E and 4-hydroxynonenal (4-HNE) depict improved histology and lipid peroxidation, respectively. Scale bar: 100  $\mu$ m. (C) Serum ALT values and (D) redox injury (lucigenin assay) show improvement, and although the (E) NADH/NAD<sup>+</sup> ratios were induced in NIAAA-treated, control virus-transduced mice, these improved significantly in *Shc<sup>HepKO</sup>* mice. (F) Liver TG values and (G) Oil red O staining show mild improvement in *Shc<sup>HepKO</sup>* mice. Scale bar: 100  $\mu$ m. (C–E)  $n = 6$ –9 mice per group. All data are presented as means  $\pm$  SEM. \* $P < .05$ , \*\* $P < .01$ , and \*\*\* $P < .001$ .

inhibition in mice on the NIAAA diet. Idebenone, a benzoquinone, was discovered to have a potent Shc inhibitory effect by directly interacting with Shc to block its phosphorylation.<sup>22</sup> Mice on the NIAAA diet were dosed with

idebenone (20 mg/kg, once daily). This group showed significantly reduced serum ALT levels (Figure 7A). The expression of inflammatory mediators Cxcl1 and F4/80 (*Adgre1*) were attenuated by idebenone (Figure 7B), and



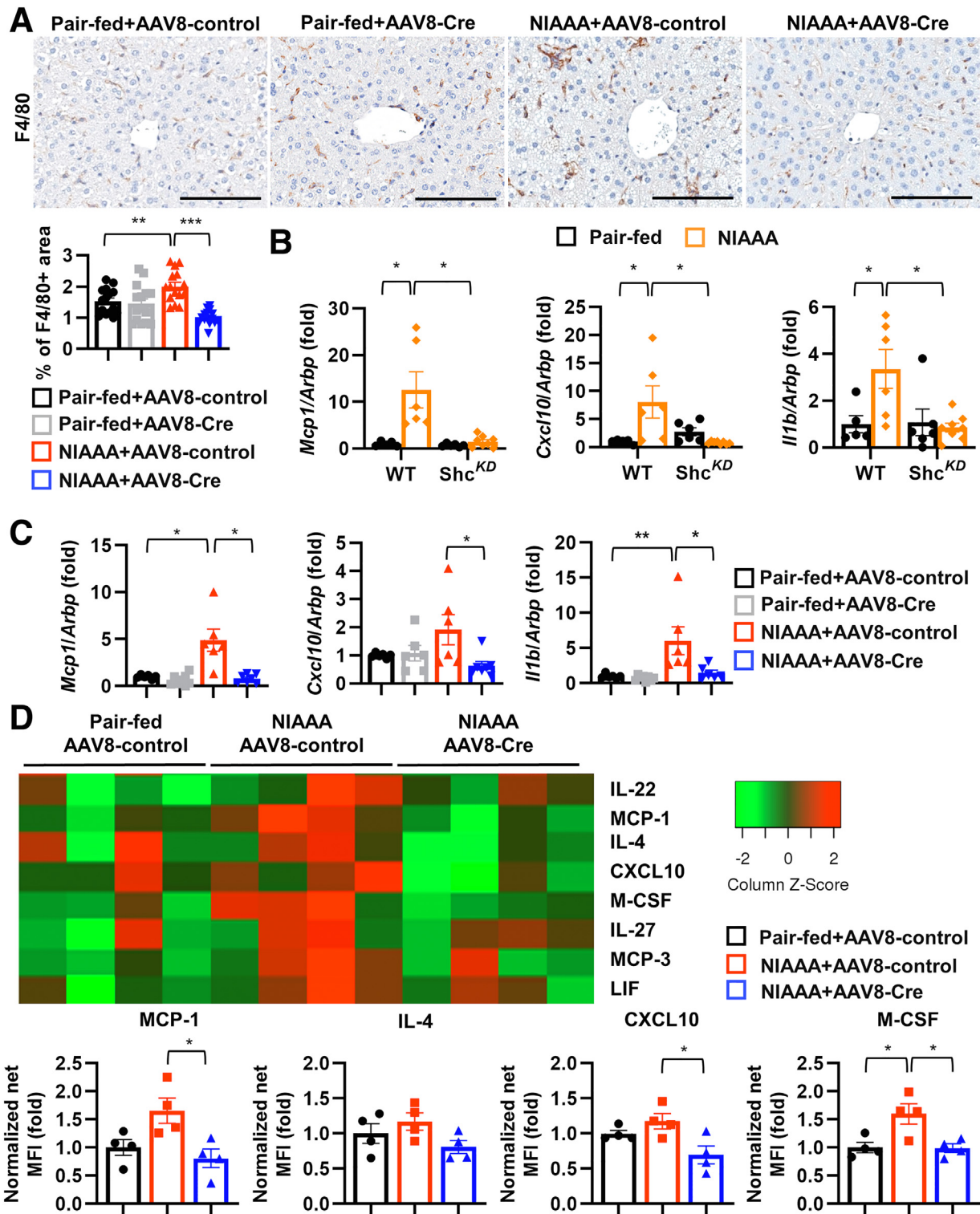


**Figure 4. *Shc*<sup>KD</sup> or *Shc*<sup>HepKO</sup> improves inflammation.** (A) Immunohistochemistry for F4/80 depicts a lower number of positive cells in livers of AAV8-cre-injected *Shc*<sup>fl/fl</sup> mice (*Shc*<sup>HepKO</sup>) on the NIAAA diet compared with AAV8-control-injected mice. Scale bar: 100  $\mu$ m. Five 20 $\times$  fields/mouse in 3 mice were counted. (B) Reverse-transcription qPCR showed NIAAA diet-induced MCP-1, CXCL10, IL1 $\beta$ , and tumor necrosis factor- $\alpha$  in WT mice, but this was attenuated in *Shc*<sup>KD</sup> mice ( $n = 5-8$ /group). (C) The NIAAA diet induced MCP-1, IL1 $\beta$ , tumor necrosis factor- $\alpha$ , and CXCL10 in control virus-transduced mice, these were attenuated in *Shc*<sup>HepKO</sup> mice, as assessed by reverse-transcription qPCR ( $n = 6$ /group). (D) Liver homogenates were analyzed by Luminex 39-plex assay and the representative heatmap is shown. Compared with pair-fed mice, most mediators were induced on the NIAAA diet, and lower levels of MCP-1, IL4, CXCL10, and macrophage colony-stimulating factor (M-CSF) were seen in *Shc*<sup>HepKO</sup> mice. All data are presented as means  $\pm$  SEM. \* $P < .05$ , \*\* $P < .01$ , and \*\*\* $P < .001$ . LIF, Leukemia inhibitory factor; MFI, median fluorescence intensity.

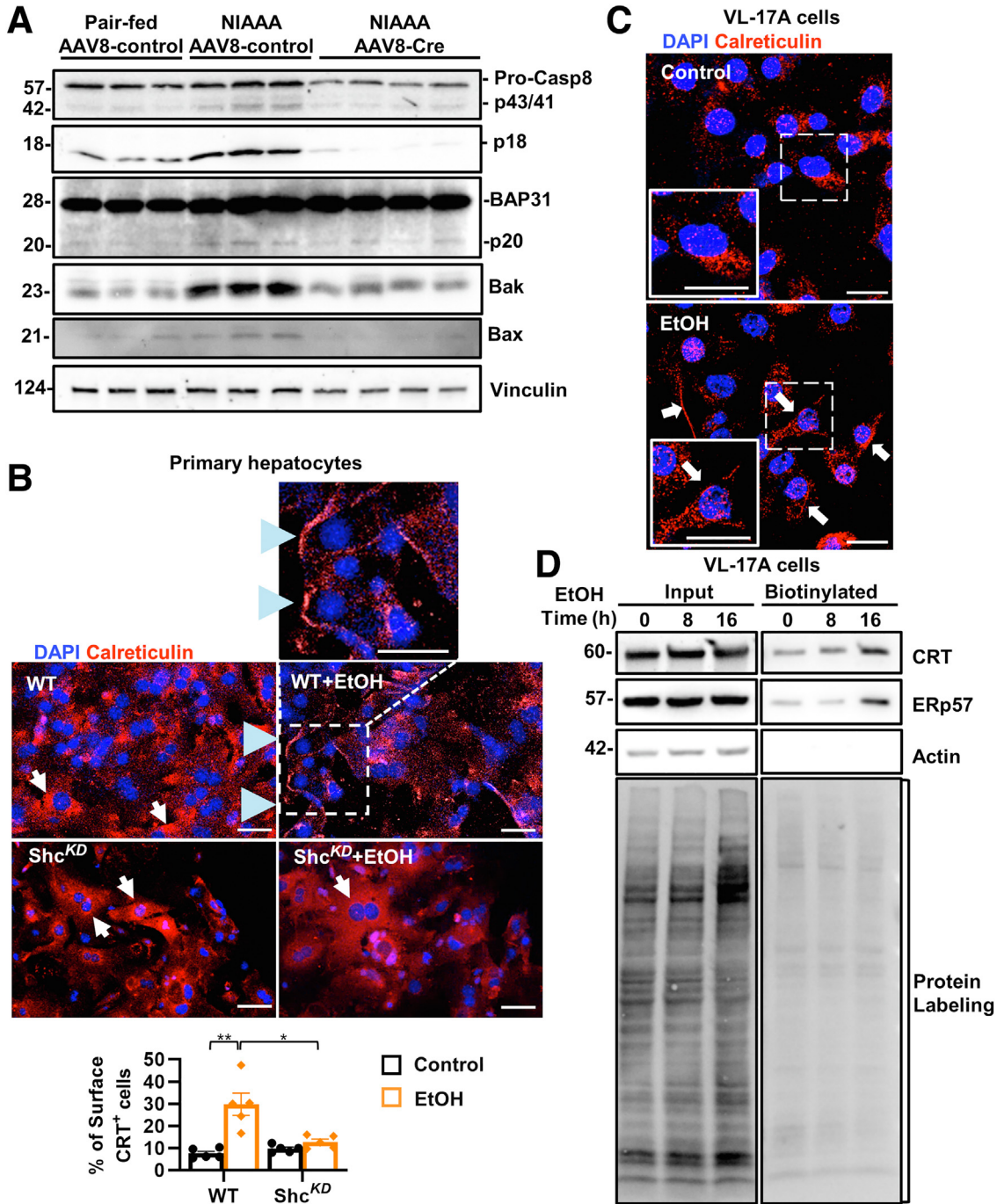


**Figure 5. Alcohol induces the translocation of CRT in a Shc-dependent manner.** (A) Western blots on liver cytosolic proteins depict cleavage of caspase-8 and BAP31 in Shc<sup>fl/fl</sup> mice on the NIAAA diet, but not in Shc<sup>HepKO</sup> mice; and Bcl2 members Bax and Bak were attenuated in Shc<sup>HepKO</sup> mice. (B) Immunofluorescence studies of primary hepatocytes isolated from control (WT) or Shc<sup>KD</sup> livers show CRT localized to the perinuclear area (indicated by white arrows) in nontreated cells (red, CRT; blue, 4',6-diamidino-2-phenylindole [DAPI]). Scale bar: 20 μm. After ethanol treatment (EtOH; 100 mmol/L for 8 hours), CRT signal was observed on the cell membrane in WT (indicated by blue arrowheads) but not in the Shc<sup>KD</sup> hepatocytes. Quantitation of the number of membrane-positive cells showed a significant increase in alcohol-treated WT cells (five 20× fields per group were counted, means ± SEM, \*P < .05, \*\*P < .01). (C) To study CRT translocation in human cells, VL-17A cells were treated with 100 mmol/L ethanol for 8 hours, and immunofluorescence was performed as described earlier. An increase in cell membrane exposure of CRT (indicated by white arrows) was seen in alcohol-treated cells (red, CRT; blue, DAPI). Scale bar: 10 μm. The surface membrane proteins of VL-17A cells were labeled with biotin after 100 mmol/L ethanol treatment for 8 or 16 hours. (D) Whole-cell lysate (input) and isolated cell surface proteins (biotinylated) were subjected to Western blot. There was an increase in cell surface CRT and ERp57 at 16 hours of alcohol exposure.



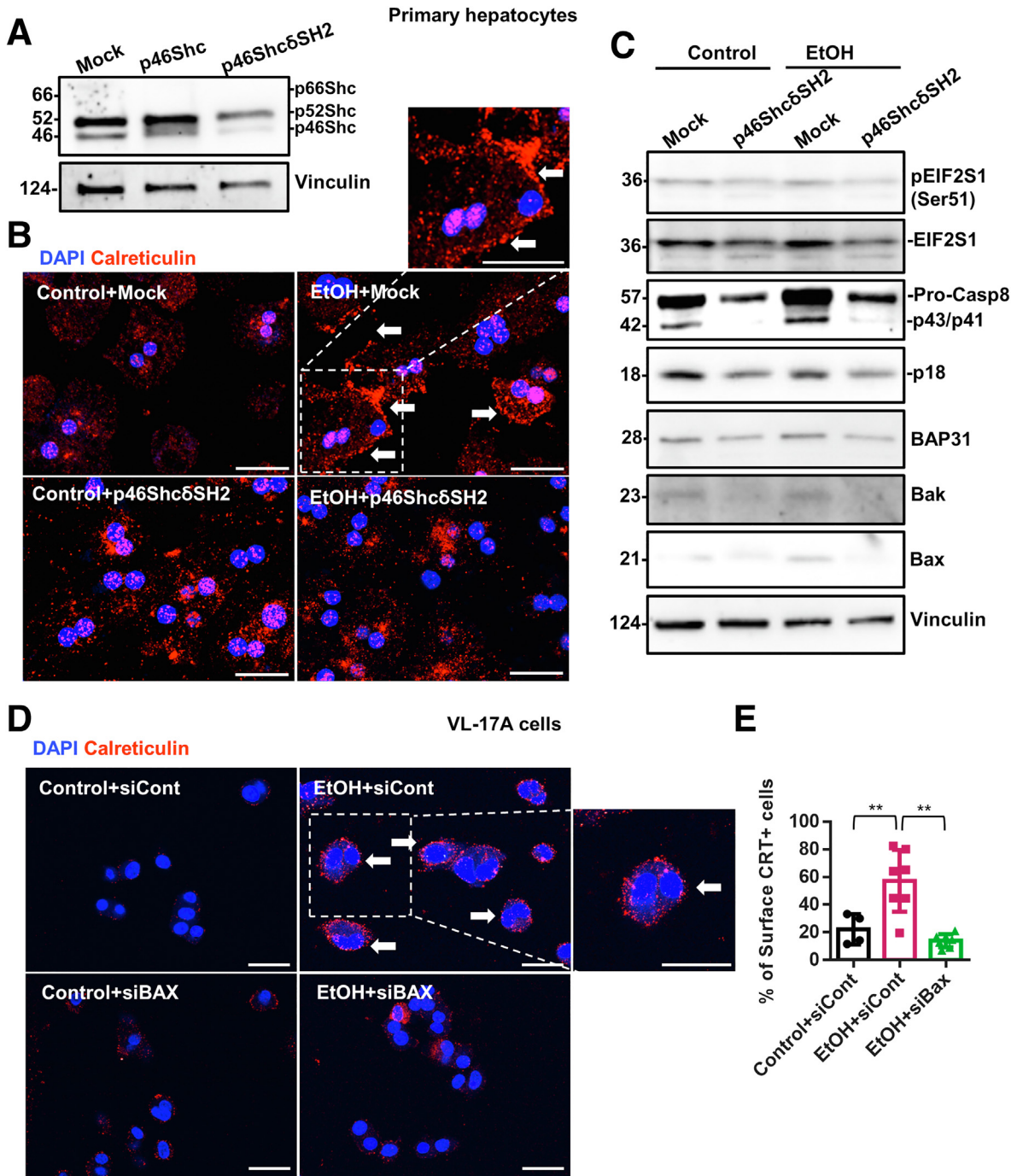


**Figure 6.** p46Shc inhibition decreases CRT cell membrane translocation and alcohol-mediated induction of eukaryotic translation initiation factor 2 subunit  $\alpha$  (EIF2S1), caspase 8 cleavage, and activation of Bak and Bax. (A) Mouse primary hepatocytes were transfected with the p46Shc $\delta$ SH2 plasmid or mock-transfected for 24 hours, exposed to alcohol (100 mmol/L for 8 hours), and immunofluorescence was performed to visualize CRT. In mock-transfected, alcohol-exposed cells, CRT showed an increased cell membrane signal (white arrows), but not in (B) p46Shc $\delta$ SH2-transfected cells (red, calreticulin; blue, 4',6-diamidino-2-phenylindole [DAPI]). Scale bar: 20  $\mu$ m. (C) In p46Shc $\delta$ SH2-transfected cells subjected to Western blot analysis, phos-EIF2S1 (Ser51), cleaved caspase 8, BAP31, Bak, and Bax were attenuated. VL-17A cells were transfected with control siRNA (siCont) or BAX siRNA (siBAX) for 24 hours, exposed to alcohol (100 mmol/L for 24 hours), and immunofluorescence was performed to visualize calreticulin. (D) In alcohol-exposed cells, CRT showed an increased cell membrane signal (white arrows) in siCont- but not in siBAX-transfected cells (red, calreticulin; blue, DAPI). Scale bar: 20  $\mu$ m. (E) The percentage of surface CRT+ cells was quantified (data are presented as means  $\pm$  SEM, n = 4–7 10 $\times$  fields per group, \*\*P < .05).



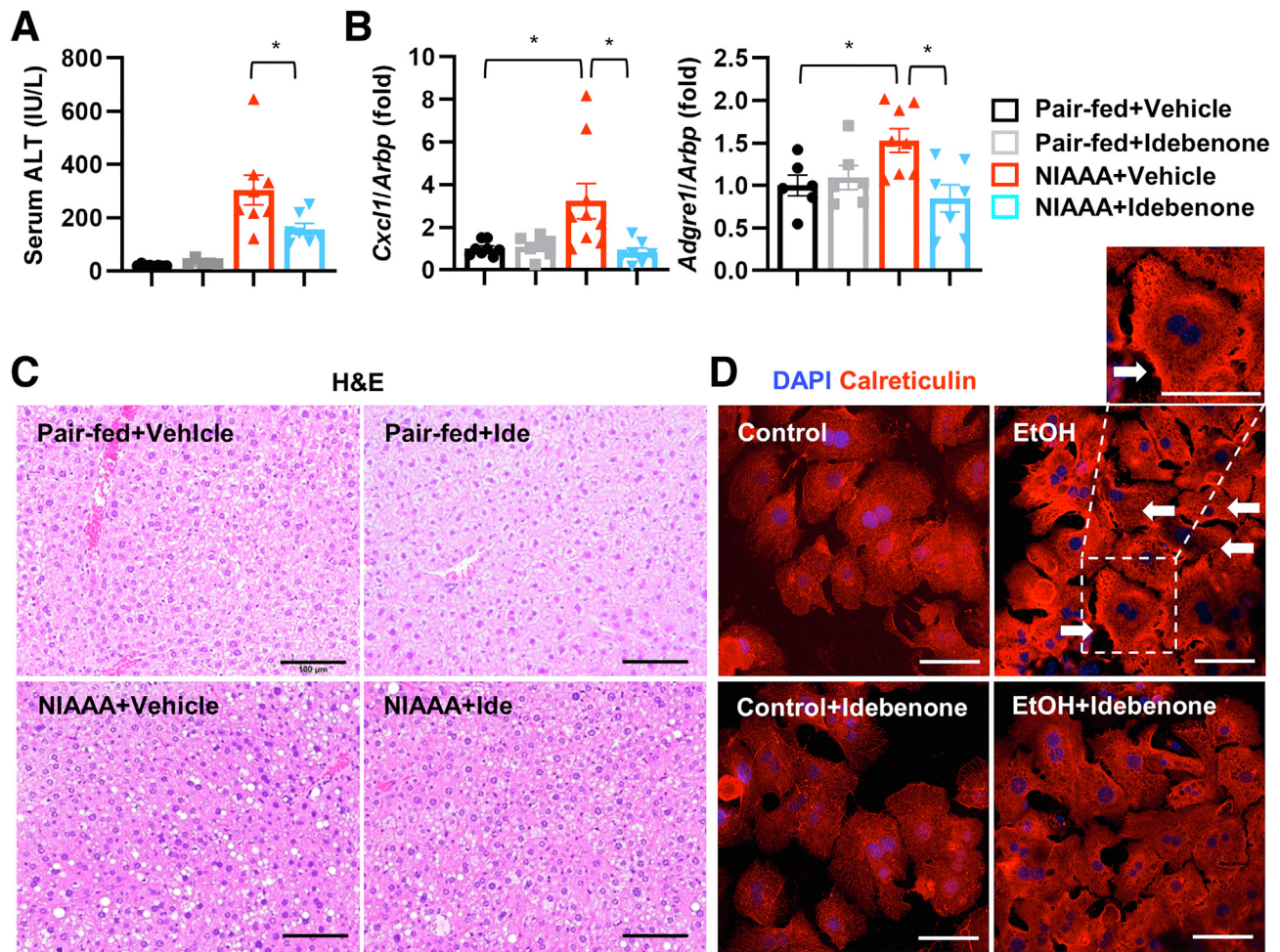


**Figure 7.** Idebenone, a Shc inhibitor, protects against alcohol-induced liver injury in vivo. Mice on an alcohol diet (NIAAA model) were treated with idebenone 20 mg/kg or vehicle once daily for 10 days. (A) Serum ALT levels were reduced significantly by idebenone ( $n = 7-8$ /group). (B) Reverse-transcription qPCR to evaluate proinflammatory transcripts showed decreased expression of CXCL1 and F4/80 (encoded by *Adgre1*) in idebenone-treated mice ( $n = 6-8$ /group). (C) H&E showed improved inflammation, and steatosis. Scale bar: 100  $\mu\text{m}$ . Primary mouse hepatocytes were treated with idebenone 10  $\mu\text{mol/L}$  for 30 minutes followed by alcohol (EtOH) 100 mmol/L, and immunofluorescence was performed to visualize CRT. (D) In alcohol-exposed cells CRT showed an increased cell membrane signal (white arrows), but not in idebenone-pretreated cells (red, CRT; blue, 4',6-diamidino-2-phenylindole [DAPI]). Scale bar: 50  $\mu\text{m}$ . All data are presented as means  $\pm$  SEM,  $n = 6-8$ . \* $P < .05$ .

liver histology improved as well (Figure 7C). In addition, in mouse primary hepatocytes, idebenone pretreatment (10  $\mu\text{mol/L}$ , 30 min) abrogated alcohol-induced CRT translocation (Figure 7D).

## Discussion

In this study we show that during alcoholic hepatitis, Shc activation, particularly the p46Shc isoform, lipid peroxidation, and CRT membrane exposure are interlinked (Figure 8). The Shc family of adapter proteins are involved in modulating redox and metabolic stress signals elicited by various stimuli, for example, receptor tyrosine kinases, or growth factor signaling. Of the 3 isoforms, the liver mainly expresses p46Shc, and p52Shc in physiological conditions, although the level of p66Shc is much lower.<sup>23</sup> In the past, most Shc-related effects were attributed to p66Shc,

however, the KO mice used in these experiments in reality were hypomorphs, having reduced levels of all 3 isoforms; therefore, the other isoforms deserve attention.<sup>3</sup> In our study, we observed that Shc was induced in patients with alcoholic hepatitis, and that feeding the NIAAA diet to mice led to increased expression of p46Shc and p52Shc. We focused on p46Shc because it is a mitochondrial isoform and was shown to bind to and inhibit the enzymatic activity of the lipid oxidation enzyme ACAA2.<sup>20</sup> Thus, it was plausible that p46Shc induction during AH could result in reduced  $\beta$ -oxidation, which in turn causes an increase in ROS and lipid peroxidation. Indeed, we found that oxidative radicals and lipid peroxidation improved in *Shc<sup>HepKO</sup>* and *Shc<sup>KD</sup>* mice fed the NIAAA diet. These effects, of course, could have been the cumulative result of reducing all isoforms because studying p46Shc-specific effects in vivo is not yet possible. We earlier showed that in nonalcoholic steatohepatitis, p52Shc could

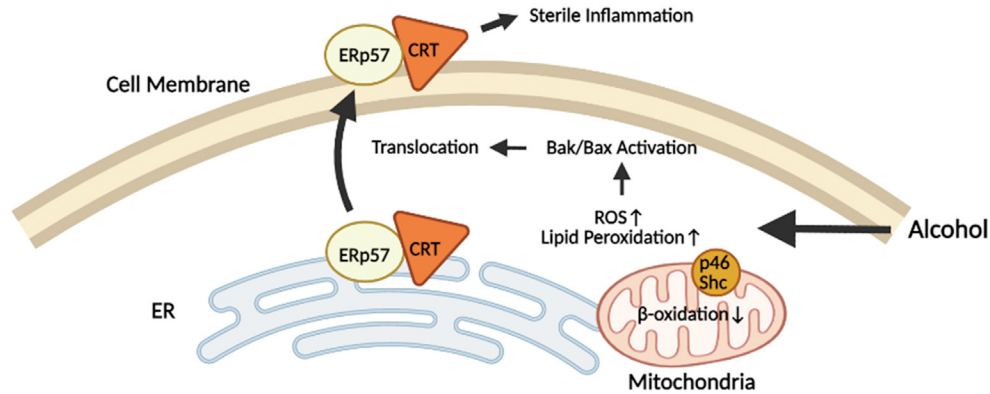


**Figure 8. Schematic depiction of the proposed role of Shc and CRT translocation in alcohol-induced injury in hepatocytes.** Shc induction during alcoholic hepatitis is linked to maladaptive responses with increased lipid peroxidation and production of ROS. Key to this is the mitochondrial p46Shc isoform that can inhibit fatty acid  $\beta$ -oxidation. Activation of eukaryotic translation initiation factor 2 subunit  $\alpha$ , pre-apoptotic signals with caspase-8 and BAP31 cleavage, and Bak/Bax activation lead to CRT/ERp57 complex translocation from the ER to the cell membrane where they act as DAMP and elicit an inflammatory response. Shc inhibition may protect hepatocytes against alcohol-induced injury. Created with [BioRender.com](https://www.biorender.com).

bind to and activate the NADPH oxidase 2 via its p47<sup>phox</sup> subunit, inducing production of ROS.<sup>23</sup> Therefore, it is conceivable that in alcoholic hepatitis not only the mitochondrial isoforms but p52Shc also plays a role in the generation of redox radicals.

Alcohol metabolism exerts a significant increase in the NADH/NAD<sup>+</sup> ratio in the mitochondria and hepatocyte cytoplasm. This is thought to be linked to a defect in  $\beta$ -oxidation, and in our case the ratio was reversed in Shc<sup>KD</sup> and Shc<sup>HepKO</sup> mice, signifying an important Shc-mediated effect. Taken together, these data point to an important maladaptive effect elicited by increased Shc in alcoholic liver disease, and furthermore detailed studies are required to decipher the effects of p46Shc on mitochondrial bioenergetics and lipid metabolism.

Alcohol-induced lipid peroxidation can result in proteostasis with an activation of ER stress.<sup>14</sup> ER stress involving eukaryotic initiation factor 2 alpha (EiF2 $\alpha$ ) activation and caspase 8-mediated BAP31 cleavage were linked to the activation of Bak and Bax in cancer cells, and depleting caspase-8, BAP31, Bax, and Bak prevented CRT/ERp57 exposure and immunogenicity.<sup>24</sup> Because both EiF2 $\alpha$  activation and pre-apoptotic signals were attenuated after p46Shc $\delta$ SH2 transfection, p46Shc is likely to be an important isoform in alcoholic injury. CRT membrane presence can signal immunogenicity even before the cells manifest real signs of apoptosis, and this could be an important feature in early injury in alcoholic hepatitis because the presence of CRT on the cytoplasmic membrane is a key signal for recognition by mononuclear cells.<sup>25</sup> We found that chemokines denoting monocyte recruitment (e.g. MCP-1, IL4, and CXCL-10) were reduced significantly in a Shc-dependent manner in both the Shc<sup>KD</sup> and Shc<sup>HepKO</sup> livers and after treatment with the Shc inhibitor. Macrophages are known to play a proinflammatory role and tissue remodeling in alcohol models.<sup>26</sup> In our study, consistently, the number of F4/80 cells increased and Shc deletion in hepatocyte and idebenone treatment reversed the effects.

Idebenone recently was discovered as a potent Shc inhibitor, albeit not isoform-specific.<sup>22</sup> For a long time idebenone was thought to be an antioxidant, however, recent data have shown potent binding activity at nanomolar concentrations to Shc.<sup>27</sup> In our study, idebenone reduced ALT/aspartate aminotransferase levels, inflammatory mediators, and CRT expression.

Taken together, in alcoholic hepatitis Shc-dependent pre-apoptotic pathways in conjunction with ER stress lead to membrane exposure of CRT/ERp57 as an important DAMP complex. Targeting Shc could be a novel therapeutic strategy mitigating liver injury in alcoholic hepatitis.

## Materials and Methods

### Human Biopsy Samples

DNA microarray data were extracted and analyzed from NCBI GSE28619.<sup>10</sup> The DNA microarray included 15 AH patients (mean patient age, 49 y) and 7 normal livers (mean patient age, 51 y). Formalin-fixed paraffin-embedded human liver biopsy samples were obtained from the University of California Davis Cancer Center Biorepository (funded by the National Cancer Institute). Samples were de-identified and exempted (exemption 4). The study protocol conformed to the ethical guidelines of the 1975 Declaration of Helsinki as reflected in a priori approval by the appropriate institutional review committee. Biopsy samples from 3 different patients were analyzed by IHC.

### Animal Studies

All animal experiments were conducted according to the experimental procedures approved by the Institutional Animal Care and Use Committee at the University of California Davis, Stanford University, and Palo Alto, Veterans Affairs. Shc hypomorph (Shc<sup>KD</sup>) mice were originally from Dr Pelicci's laboratory.<sup>28</sup> Shc<sup>f/f</sup> mice were gifted by Dr Fawaz Haj (University of California Davis, Davis, CA). Genotypes of the progenies were confirmed as previously described.<sup>1,29</sup> Mice were



housed in standard cages with 12:12-hour light/dark cycles and ad libitum access to water and food unless otherwise indicated. Chronic plus binge alcohol treatment was given as per the NIAAA protocol.<sup>30</sup> In brief, all mice first were acclimated to the 5-day Lieber-DeCarli control liquid diet (F1259SP; Bio-Serv). Mice in the alcohol (NIAAA) group were subjected to 10-day 5% v/v ethanol (BP2818-500; Fisher Scientific)-containing liquid diet (F1258SP; Bio-Serv) and an acute ethanol binge (5 g/kg body weight) on the 11th day, and mice in the control (pair-fed) group were fed with a control liquid diet and binged with maltose dextrin in a calorie-matched manner. In the first cohort, 14-week-old Shc<sup>KD</sup> mice and age-matched Shc<sup>f/f</sup> (WT) mice were placed on the NIAAA diet model or subjected to hepatocyte isolation. In the second cohort, 14-week-old male Shc<sup>f/f</sup> mice were assigned to the NIAAA group or the pair-fed group in an age-matched version, and were injected intravenously with either AAV8-control green fluorescent protein (AAV8-control) or AAV8-thyroxine-binding globulin-Cre recombinase (AAV8-Cre) on day 5 of the 10-day diet to generate Shc<sup>HepKO</sup> mice ( $5 \times 10^{11}$  genome copies; Vector BioLabs), and the rationale of the specific deletion in hepatocytes has been reported previously.<sup>31</sup> In the third cohort, 10-week-old C57BL6 mice (Jackson Laboratory) were assigned to the NIAAA group or the pair-fed group and dosed with idebenone (I5659; MilliporeSigma) as previously described.<sup>22</sup> In brief, mice were acclimated before the 10-day NIAAA diet started, then were fed either 0.11 g peanut butter (vehicle group, idebenone's absorption is increased by foods high in lipids) or idebenone formulated in 0.11 g of peanut butter (20 mg/kg body weight, idebenone group) once daily for 10 days. Mice were observed eating all the peanut butter.

### Cell Culture

Primary mouse hepatocytes were isolated after collagenase reverse perfusion as described previously.<sup>32</sup> The cells were maintained in William's E medium (W4125; Sigma-Aldrich) supplemented with 10% fetal bovine serum (10437028; Gibco) and antibiotics (15240062; Gibco). VL-17A cells were gifted by Dr Wen-Xing Ding (University of Kansas Medical Center) and Dr Dahn Clemens (University of Nebraska Medical Center, Omaha, NE), selected by G418 (10131035; Gibco) and Zeocin (R25001; Invitrogen), and cultured in Dulbecco's modified Eagle medium (11995073; Gibco) supplemented with 10% fetal bovine serum and antibiotics.

### Cell Transfection, Plasmids, and Small Interfering RNAs

Plasmids containing human WT p46Shc and deletion-mutant p46Shc $\delta$ SH2 were constructed and confirmed.<sup>20</sup> The SH2 domain was deleted using forward primer 5'-GAGCTGCTCAGCCATGGACAC-3' and reverse primer 5'-GAGCGGAAACTGTACCTCGAGT-3', and EX-H9090-M62-p46Shc $\delta$  (329-425) SH2 was constructed. Primary hepatocytes were transfected with 2  $\mu$ g DNA per 12 wells or 3  $\mu$ g DNA per 6 wells for approximately 24 hours using the jetPEI-Hepatocyte DNA transfection reagent (89129-944; Polyplus) following the manufacturer's instruction. BAX small

interfering RNA (siRNA) (sc-29212) and control siRNA (sc-37007) were from Santa Cruz Biotechnology, Inc, and the transfection was performed using Lipofectamine 3000 Transfection Reagent (L3000001; Invitrogen) according to the manufacturer's instructions. Briefly, VL-17A cells were seeded on a collagen-coated, 8-well, chambered glass slide and incubated with 10 pm BAX or control siRNA and 1  $\mu$ L Lipofectamine 3000 reagent in serum-free medium for 24 hours.

### Serum ALT Measurement

Mouse blood was collected at the time of death and centrifuged at  $8000 \times g$  at room temperature for 10 minutes twice. The supernatant was collected as serum, aliquoted, and snap-frozen. ALT and aspartate aminotransferase levels were measured by the University of California Davis Comparative Pathology Laboratory or the Diagnostic Laboratory at Stanford Department of Comparative Medicine.

### Liver TG Measurement

Frozen liver tissue (20–50 mg) was homogenized in 1 mL chloroform/methanol (v/v = 2:1) with vigorous shaking for 1 hour at room temperature. Subsequently, 200  $\mu$ L Millipore water was added into the mix and centrifuged at  $3000 \times g$  for 5 minutes. The lower lipid phase was collected and dried in a fume hood overnight, and the pellet was dissolved in 60  $\mu$ L tert-butanol and 40  $\mu$ L Triton X-114 (Thermo)/methanol (v/v = 2:1) mix. Liver TG levels were measured with colorimetric assay kits, following the manufacturer's instructions (Pointe Scientific, Canton, MI), and normalized to tissue weight. The tert-butanol and Triton X-114/methanol mixture was used as a blank control.

### RNA Extraction, Reverse Transcription, and Real-Time qPCR

Total RNA was isolated from snap-frozen liver tissue and cells as per the manufacturer's instructions using the RNeasy mini kit (74104; Qiagen). Equal concentration of RNA was used to synthesize complementary DNA using the iScript complementary DNA synthesis kit (1708891; Bio-Rad). Reverse-transcription qPCR was performed using Power SYBR Green PCR Master Mix (4368706; Applied Biosystems) on the 7900HT system (Applied Biosystems), and the results were analyzed by the delta-delta cycle threshold ( $2^{-\Delta\Delta C_t}$ ) method. The results were normalized with acidic ribosomal phosphoprotein (*Arbp*) as endogenous control. The primer sequences used in this study are listed in Table 1.

### Protein Extraction and Western Blot

Frozen liver tissue samples were homogenized and lysed with radioimmunoprecipitation buffer (10 mmol/L Tris-HCl, 1 mmol/L EDTA, 0.5 mmol/L ethylene glycol-bis( $\beta$ -aminoethyl ether)-*N,N,N',N'*-tetraacetic acid, 1% Triton X-100, 0.1% sodium deoxycholate, 0.1% sodium dodecyl sulfate [SDS], and 140 mmol/L NaCl). The homogenate was centrifuged and the supernatant was collected for Western

**Table 1.** Sequence of Primers Used in This Study

Messenger RNA	Primer sequence
Mouse <i>Arbp</i>	Forward: 5'-CAAAGCTGAAGCAAAGGAAGAG-3' Reverse: 5'-AATTAAGCAGGCTGACTTGGTTG-3'
Mouse <i>calreticulin</i>	Forward: 5'-CCTGCCATCTATTCAAAGAGCA-3' Reverse: 5'-GCATCTTGGCTTGCTGCAA-3'
Mouse <i>Cxcl1</i>	Forward: 5'-ACCGAAGTCATAGCCACACT-3' Reverse: 5'-TCTGAACCAAGGGAGCTTCA-3'
Mouse <i>Cxcl10</i>	Forward: 5'-CAGTGAGAATGAGGGCCATAG-3' Reverse: 5'-TTCTTGATGGTCTTAGATTCCGG-3'
Mouse <i>Adgre1</i>	Forward: 5'-TGTAAGTGAAGTCAAGGACT-3' Reverse: 5'-ATGAAGGTGGGACCACAGAG-3'
Mouse <i>Il1β</i>	Forward: 5'-CAACCAACAAGTGATATTCTCCATG-3' Reverse: 5'-GATCCACACTCTCCAGCTGCA-3'
Mouse <i>Mcp1</i>	Forward: 5'-CTTCTGGGCTGCTGTTCA-3' Reverse: 5'-CCAGCCTACTCATTGGGATCA-3'

blot. Cells were washed with phosphate-buffered saline (PBS) and lysed with Cell Lysis Buffer (9803; Cell Signaling Technology). The homogenate was centrifuged and the supernatant was collected. Protein concentration was determined with the Bio-Rad Protein Assay Kit (5000001; Bio-Rad) or the Pierce BCA Protein Assay Kit (23225; Thermo). Protease inhibitor (4693116001; Roche) and phosphatase inhibitor (4906837001; Roche) were added to all the lysis procedures mentioned previously, and 10–50 μg of the protein samples were loaded onto SDS-polyacrylamide gel. The proteins were transferred to a polyvinylidene difluoride membrane or nitrocellulose membrane that was blocked with 5% bovine serum albumin in Tris-buffered saline with 0.1% Tween 20 (v/v) and then incubated with primary antibodies at 4°C (Table 2) overnight. The blots were washed with Tris-buffered saline with

0.1% Tween 20 (v/v) and further incubated with horseradish-peroxidase-conjugated secondary antibodies (Table 3). Signal was detected by adding Western-Bright enhanced chemiluminescence substrate (K-12045-D20; Advansta, Menlo Park, CA) or SuperSignal West Pico PLUS Chemiluminescent Substrate (34596; Thermo) and imaged with film or the iBright CL1500 imaging system (Thermo). The images were processed and analyzed with ImageJ (National Institutes of Health, Bethesda, MD) and iBright Analysis software (Thermo).

### Histology, Immunohistochemistry, Immunofluorescence, and Oil Red O staining

Paraffin-embedded tissue samples were cut into 5-μm sections, deparaffinized, and rehydrated. For antigen retrieval, slides were boiled in citrate buffer (0.01 mol/L, pH 6.0) using a microwave oven on high power for 5 minutes and cooled down to room temperature. After incubation in 3% aqueous H<sub>2</sub>O<sub>2</sub> to quench the endogenous peroxidase, sections were washed in PBS with 0.1% Tween 20, v/v (PBST) washing buffer, blocked with 5% goat serum (566380; EMD Millipore) diluted in PBST at room temperature for 1 hour, and incubated with primary antibody (Table 2) diluted in 2% goat serum in PBST at 4°C overnight. All slides were scanned with a Leica Aperio AT2 (Leica) at Stanford Human Pathology/Histology Service Center. Images were processed with ImageJ.

For immunohistochemistry, slides were incubated with the appropriate biotinylated secondary antibodies (Table 3) for 1 hour, and then with the ABC Peroxidase Standard Staining Kit (32050; Thermo) for 30 minutes. The slides were stained with 3, 3' diaminobenzidine (ab64238; Abcam) for 5 seconds to 5 minutes and counterstained with hematoxylin (72704; Thermo) for 45 seconds. For immunofluorescence on tissues, slides were incubated with Alexa Fluor secondary antibodies (Table 3) at room temperature for 1

**Table 2.** List of Primary Antibodies Used for Various Applications in the Study

Primary antibodies	Manufacturer/catalog number	Application/concentration
4-hydroxynonenal	Abcam, ab46545	IHC, 1:500
Actin	Santa Cruz, sc47778	WB, 1:2000
Bak	Abcam, ab104124	WB, 1:1000
BAP31	Abcam, ab109304	WB, 1:1000
Bax	Abcam, ab32503	WB, 1:1000
Bax	BD Biosciences, 556467	WB: 1:500
Calreticulin	Abcam, ab2907	WB: 1:1000; IF: 1:250; FACS: 1:500
Caspase-8	Cell Signaling Technology, 4927S	WB, 1:1000
Cleaved caspase-8	Cell Signaling Technology, 8592S	WB, 1:1000
ERp57	Abcam, ab13506	WB, 1:1000
Shc	BD Biosciences, 610878	WB, 1:1000
Shc (EP332Y)	Abcam, ab33770	IHC, 1:100
Glyceraldehyde-3-phosphate dehydrogenase	Invitrogen, PA 1-988	WB, 1:1000
Vinculin	Abcam, ab129002	WB, 1:10,000

FACS, fluorescence-activated cell sorter; IF, Immunofluorescence; WB, Western blot.



**Table 3.** List of Secondary Antibodies Used in the Study

Secondary antibodies	Manufacturer/catalog number	Application/concentration
HRP goat $\alpha$ -mouse	EMD Millipore, 710453	WB, 1:5000
HRP goat $\alpha$ -rabbit	Abcam, ab6721	WB, 1:5000
Alexa Fluor 555 donkey $\alpha$ -rabbit	Invitrogen, A31572	IF, 1:500
Biotinylated goat $\alpha$ -mouse	Vector Laboratories, BA-9200	IHC, 1:500
Biotinylated goat $\alpha$ -rabbit	Vector Laboratories, BA-1000	IHC, 1:500

HRP, horseradish peroxidase; IF, immunofluorescence; WB, Western blot.

hour. Slides were washed with PBST between incubations and mounted with antifade mounting medium with 4',6-diamidino-2-phenylindole (H-1200; Vector Laboratories). Fluorescent images were taken with a Leica TCS SPE (Leica) at the Stanford Cell Sciences Imaging Facility (supported by NIH SIG 1S100D010558001A1).

Oil red O staining was performed on cryosections from fresh liver tissues embedded and frozen in optimal cutting temperature compound (Scigen). The slides were fixed in 10% neutral buffered formalin (Research Products International) for 30 minutes. After washing with water, the slides were placed in 100% propylene glycol (Poly Scientific) for 5 minutes and 85% propylene glycol for another 5 minutes. The slides were stained for Oil red O stain (Frontier Scientific) preheated at 60°C for 10 minutes, and differentiated in 85% propylene glycol for 3 minutes. The slides were counterstained with Harris Hematoxylin stain for 30 seconds, and bluing solution for 10 dips.

### Fluorescent Immunocytochemistry

Primary hepatocytes were plated on collagen-coated coverslips. After treatment, cells were washed twice with PBS and fixed with 4% paraformaldehyde at 4°C overnight. Cells were permeabilized in PBS with 0.4% (v/v) Triton X-100 for 10 minutes. After blocking with 5% goat serum in PBST at room temperature for 1 hour, cells were incubated with primary antibodies (Table 2) diluted in 2% goat serum in PBST at 4°C overnight. The following morning the slides were washed and then incubated with secondary antibodies (Table 3) at room temperature for 1 hour.

For surface staining, cells were washed with PBS twice, fixed with 0.25% paraformaldehyde for 5 minutes, and incubated with primary antibodies and with secondary antibodies for 30 minutes, respectively. Coverslips were washed with PBST between incubations and mounted with anti-fade mounting medium with 4',6-diamidino-2-phenylindole. Fluorescent images were taken with a Leica TCS SPE. Images were processed with ImageJ.

### NADH/NAD Assays

Snap-frozen liver tissue samples were processed with the NADH/NAD assay kit (ab65348; Abcam) as per the manufacturer's protocol. Briefly, total NAD (including NAD<sup>+</sup> and NADH) were extracted from liver tissues with extracting buffer. An equal amount of protein was subjected to the assay.

### Lucigenin Assay

A lucigenin assay was performed as described previously.<sup>33</sup> Snap-frozen livers were homogenized on ice in sucrose buffer (0.3 mol/L sucrose, 10 mmol/L HEPES, 10 mmol/L KCl, 0.1 mmol/L EDTA, 0.1 mmol/L ethylene glycol-bis( $\beta$ -aminoethyl ether)-*N,N,N',N'*-tetraacetic acid, 0.5 mmol/L spermidine, and 1 mmol/L dithiothreitol, pH 7.4) with protease inhibitor, and centrifuged at 1000  $\times g$  for 5 minutes. The supernatant was centrifuged further at 100,000  $\times g$  for 1 hour at 4°C to obtain membrane-enriched fractions. The pellet was suspended in Krebs buffer (100 mmol/L NaCl, 5 mmol/L KCl, 2 mmol/L CaCl<sub>2</sub>, 1.2 mmol/L MgSO<sub>4</sub>, 1.0 mmol/L K<sub>2</sub>HPO<sub>4</sub>, 25 mmol/L NaHCO<sub>3</sub>, 20 mmol/L Na-HEPES, and 0.2% glucose, pH 7.4) with protease inhibitor and incubated at 37°C for 30 minutes. Membrane fractions were incubated with 10  $\mu$ mol/L lucigenin (L6868; Invitrogen) at room temperature for 15 minutes. Then, 100  $\mu$ mol/L NADPH (Sigma-Aldrich) was added and the chemiluminescence intensity was read with a Pharmingen Monolight 3010 luminometer (BD Biosciences) every minute, for up to 10 counts. Data were normalized to the protein concentration.

### Luminex 39-Plex Cytokine Assay

Frozen mouse livers were homogenized and the same protein concentrations were solubilized in radio-immunoprecipitation buffer supplemented with protease inhibitor. Luminex cytokine measurement was performed by the Immunoassay Team at the Human Immune Monitoring Center at Stanford University. The Mouse 39-Plex Procarta kit (Thermo) was used according to the manufacturer's recommendations with slight modifications. Net median fluorescent intensity was used to generate heatmaps and to perform statistical analysis.

### Surface Protein Isolation and Biotinylation

For surface protein isolation, cells were plated and processed using the Pierce Cell Surface Protein Isolation Kit (89881; Thermo) following the manufacturer's instructions. In brief, cells were labeled with EZ-Link Sulfo-NHS-SS-Biotin, lysed, protease inhibitor and phosphatase inhibitor were added (input), isolated with NeutrAvidin Agarose column, and eluted with SDS sample buffer (161747; Bio-Rad) containing 50 mmol/L dithiothreitol eluate. Samples were subjected to Western blot as described earlier. No-

Stain Protein Labeling Reagent (A44449; Invitrogen) was added as control.

### Statistical Analysis

Data are presented as means  $\pm$  SEM. Statistical analyses were performed with GraphPad Prism 8.1.2 (GraphPad Software, San Diego, CA) using an unpaired *t* test with Welch correction or the Mann–Whitney test for nonparametric values. Normality distribution was assessed with the Kolmogorov–Smirnov test. A *P* value of at least  $<.05$  has been considered and stated as significant.

All authors had access to the study data and reviewed and approved the final manuscript.

### References

- Migliaccio E, Giorgio M, Mele S, Pelicci G, Reboldi P, Pandolfi PP, Lanfrancone L, Pelicci PG. The p66shc adaptor protein controls oxidative stress response and life span in mammals. *Nature* 1999;402:309–313.
- Saucier C, Papavasiliou V, Palazzo A, Naujokas MA, Kremer R, Park M. Use of signal specific receptor tyrosine kinase oncoproteins reveals that pathways downstream from Grb2 or Shc are sufficient for cell transformation and metastasis. *Oncogene* 2002;21:1800–1811.
- Tomilov AA, Ramsey JJ, Hagopian K, Giorgio M, Kim KM, Lam A, Migliaccio E, Lloyd KC, Berniakovich I, Prolla TA, Pelicci P, Cortopassi GA. The Shc locus regulates insulin signaling and adiposity in mammals. *Aging Cell* 2011;10:55–65.
- Koch OR, Fusco S, Ranieri SC, Maulucci G, Palozza P, Larocca LM, Cravero AAM, Farre SM, De Spirito M, Galeotti T, Pani G. Role of the life span determinant P66shcA in ethanol-induced liver damage. *Lab Invest* 2008;88:750–760.
- Perrini S, Tortosa F, Natalicchio A, Pacelli C, Cignarelli A, Palmieri VO, Caccioppoli C, Stefano FD, Porro S, Leonardini A, Ficarella R, Fazio MD, Cocco T, Puglisi F, Laviola L, Palasciano G, Giorgino F. The p66Shc protein controls redox signaling and oxidation-dependent DNA damage in human liver cells. *Am J Physiol Gastrointest Liver Physiol* 2015;309:G826–G840.
- Kubes P, Mehal WZ. Sterile inflammation in the liver. *Gastroenterology* 2012;143:1158–1172.
- Obeid M, Tesniere A, Ghiringhelli F, Fimia GM, Apetoh L, Perfettini J-L, Castedo M, Mignot G, Panaretakis T, Casares N, Métévier D, Larochette N, van Endert P, Ciccocanti F, Piacentini M, Zitvogel L, Kroemer G. Calreticulin exposure dictates the immunogenicity of cancer cell death. *Nat Med* 2007;13:54–61.
- Comba A, Bonnet LV, Goitea VE, Hallak ME, Galiano MR. Arginylated calreticulin increases apoptotic response induced by bortezomib in glioma cells. *Mol Neurobiol* 2019;56:1653–1664.
- Giglio P, Gagliardi M, Tumino N, Antunes F, Smaili S, Cotella D, Santoro C, Bernardini R, Mattei M, Piacentini M, Corazzari M. PKR and GCN2 stress kinases promote an ER stress-independent eIF2 $\alpha$  phosphorylation responsible for calreticulin exposure in melanoma cells. *Oncoimmunology* 2018;7:e1466765.
- Affo S, Dominguez M, Lozano JJ, Sancho-Bru P, Rodrigo-Torres D, Morales-Ibanez O, Moreno M, Millan C, Loaeza-del-Castillo A, Altamirano J, Garcia-Pagan JC, Arroyo V, Gines P, Caballeria J, Schwabe RF, Bataller R. Transcriptome analysis identifies TNF superfamily receptors as potential therapeutic targets in alcoholic hepatitis. *Gut* 2013;62:452–460.
- Bertola A, Mathews S, Ki SH, Wang H, Gao B. Mouse model of chronic and binge ethanol feeding (the NIAAA model). *Nat Protoc* 2013;8:627–637.
- Zakhari S, Li TK. Determinants of alcohol use and abuse: impact of quantity and frequency patterns on liver disease. *Hepatology* 2007;46:2032–2039.
- Obeid M, Tesniere A, Ghiringhelli F, Fimia GM, Apetoh L, Perfettini JL, Castedo M, Mignot G, Panaretakis T, Casares N, Métévier D, Larochette N, van Endert P, Ciccocanti F, Piacentini M, Zitvogel L, Kroemer G. Calreticulin exposure dictates the immunogenicity of cancer cell death. *Nat Med* 2007;13:54–61.
- Ji C, Kaplowitz N. Betaine decreases hyperhomocysteinemia, endoplasmic reticulum stress, and liver injury in alcohol-fed mice. *Gastroenterology* 2003;124:1488–1499.
- Petrasek J, Iracheta-Vellve A, Csak T, Satishchandran A, Kodys K, Kurt-Jones EA, Fitzgerald KA, Szabo G. STING-IRF3 pathway links endoplasmic reticulum stress with hepatocyte apoptosis in early alcoholic liver disease. *Proc Natl Acad Sci U S A* 2013;110:16544–16549.
- Kepp O, Semeraro M, Bravo-San Pedro JM, Bloy N, Buqué A, Huang X, Zhou H, Senovilla L, Kroemer G, Galluzzi L. eIF2 $\alpha$  phosphorylation as a biomarker of immunogenic cell death. *Semin Cancer Biol* 2015;33:86–92.
- Panaretakis T, Kepp O, Brockmeier U, Tesniere A, Bjorklund AC, Chapman DC, Durchschlag M, Joza N, Pierron G, van Endert P, Yuan J, Zitvogel L, Madeo F, Williams DB, Kroemer G. Mechanisms of pre-apoptotic calreticulin exposure in immunogenic cell death. *EMBO J* 2009;28:578–590.
- Donohue TM, Osna NA, Clemens DL. Recombinant Hep G2 cells that express alcohol dehydrogenase and cytochrome P450 2E1 as a model of ethanol-elicited cytotoxicity. *Int J Biochem Cell Biol* 2006;38:92–101.
- Panaretakis T, Joza N, Modjtahedi N, Tesniere A, Vitale I, Durchschlag M, Fimia GM, Kepp O, Piacentini M, Froehlich KU, van Endert P, Zitvogel L, Madeo F, Kroemer G. The co-translocation of ERp57 and calreticulin determines the immunogenicity of cell death. *Cell Death Differ* 2008;15:1499–1509.
- Tomilov A, Tomilova N, Shan Y, Hagopian K, Bettaieb A, Kim K, Pelicci PG, Haj F, Ramsey J, Cortopassi G. p46Shc inhibits thiolase and lipid oxidation in mitochondria. *J Biol Chem* 2016;291:12575–12585.
- Moon KH, Hood BL, Kim BJ, Hardwick JP, Conrads TP, Veenstra TD, Song BJ. Inactivation of oxidized and S-nitrosylated mitochondrial proteins in alcoholic fatty liver of rats. *Hepatology* 2006;44:1218–1230.
- Tomilov A, Allen S, Hui CK, Bettaieb A, Cortopassi G. Idenone is a cytoprotective insulin sensitizer whose



- mechanism is Shc inhibition. *Pharmacol Res* 2018; 137:89–103.
23. Jiang JX, Fish SR, Tomilov A, Li Y, Fan W, Dehnad A, Gae D, Das S, Mozes G, Charville GW, Ramsey J, Cortopassi G, Torok NJ. Non-phagocytic activation of NOX2 is implicated in progressive non-alcoholic steatohepatitis during aging. *Hepatology* 2020;72:1204–1218.
  24. Bezu L, Sauvat A, Humeau J, Gomes-da-Silva LC, Iribarren K, Forveille S, Garcia P, Zhao L, Liu P, Zitvogel L, Senovilla L, Kepp O, Kroemer G. eIF2 $\alpha$  phosphorylation is pathognomonic for immunogenic cell death. *Cell Death Differ* 2018;25:1375–1393.
  25. Chao MP, Jaiswal S, Weissman-Tsukamoto R, Alizadeh AA, Gentles AJ, Volkmer J, Weiskopf K, Willingham SB, Raveh T, Park CY, Majeti R, Weissman IL. Calreticulin is the dominant pro-phagocytic signal on multiple human cancers and is counterbalanced by CD47. *Sci Transl Med* 2010;2:63ra94.
  26. Ju C, Mandrekar P. Macrophages and alcohol-related liver inflammation. *Alcohol Res* 2015;37:251–262.
  27. Gueven N, Ravishankar P, Eri R, Rybalka E. Idebenone: when an antioxidant is not an antioxidant. *Redox Biol* 2021;38:101812.
  28. Giorgio M, Berry A, Berniakovich I, et al. The p66Shc knocked out mice are short lived under natural condition. *Aging Cell* 2012;11:162–168.
  29. Jiang JX, Fish SR, Tomilov A, Li Y, Fan W, Dehnad A, Gae D, Das S, Mozes G, Charville GW, Ramsey J, Cortopassi G, Török NJ. Nonphagocytic activation of NOX2 is implicated in progressive nonalcoholic steatohepatitis during aging. *Hepatology* 2020; 72:1204–1218.
  30. Bertola A, Mathews S, Ki SH, Wang H, Gao B. Mouse model of chronic and binge ethanol feeding (the NIAAA model). *Nat Protoc* 2013;8:627–637.
  31. Yan Z, Yan H, Ou H. Human thyroxine binding globulin (TBG) promoter directs efficient and sustaining transgene expression in liver-specific pattern. *Gene* 2012; 506:289–294.
  32. Kodama Y, Kisseleva T, Iwaisako K, Miura K, Taura K, De Minicis S, Osterreicher CH, Schnabl B, Seki E, Brenner DA. c-Jun N-terminal kinase-1 from hematopoietic cells mediates progression from hepatic steatosis to steatohepatitis and fibrosis in mice. *Gastroenterology* 2009;137:1467–1477.e5.
  33. Sasaki Y, Dehnad A, Fish S, Sato A, Jiang J, Tian J, Schröder K, Brandes R, Török NJ. NOX4 regulates CCR2 and CCL2 mRNA stability in alcoholic liver disease. *Sci Rep* 2017;7:46144.
- 
- Received October 29, 2021. Accepted September 12, 2022.**
- Correspondence**  
Address correspondence to: Natalie J. Török, MD, MSc, Division of Gastroenterology and Hepatology, Stanford School of Medicine, 300 Pasteur Drive, Alway Building Room M207, Stanford, California 94305. e-mail: ntorok@stanford.edu.
- Acknowledgments**  
The authors are grateful to Dr Fawaz Haj (Department of Nutrition, University of California Davis) for the Shc *fl/fl* mice, and to Dr Wen-Xin Ding (Pharmacology, Toxicology and Therapeutics, University of Kansas Medical Center) for the VL-17A cells. The authors also thank Jonathan Van Dyke for technical assistance.
- CRedit Authorship Contributions**  
Yuan Li (Data curation: Equal; Formal analysis: Equal; Investigation: Equal; Visualization: Lead; Writing – original draft: Equal; Writing – review & editing: Supporting)  
Joy X. Jiang (Data curation: Equal; Formal analysis: Supporting; Investigation: Equal; Writing – review & editing: Supporting)  
Weiguo Fan (Investigation: Supporting)  
Sarah R. Fish (Formal analysis: Supporting; Investigation: Equal)  
Suvarthi Das (Investigation: Equal; Writing – original draft: Supporting)  
Parul Gupta (Investigation: Supporting)  
Gergely Mozes (Investigation: Supporting)  
Lorand Vancza (Methodology: Supporting)  
Sutapa Sarkar (Investigation: Supporting)  
Koshi Kunimoto (Investigation: Supporting)  
Dongning Chen (Methodology: Supporting)  
Hyesuk Park (Investigation: Supporting)  
Dahn Clemens (Resources: Supporting; Writing – review & editing: Supporting)  
Alexey Tomilov (Resources: Supporting; Writing – review & editing: Supporting)  
Gino Cortopassi (Funding acquisition: Supporting; Resources: Supporting; Supervision: Supporting; Writing – review & editing: Supporting)  
Natalie J. Torok (Conceptualization: Lead; Funding acquisition: Lead; Resources: Lead; Supervision: Lead; Writing – original draft: Lead; Writing – review & editing: Lead)
- Conflicts of interest**  
The authors disclose no conflicts.
- Funding**  
Supported by Veterans Affairs merit awards I01 BX002418 and 5RO1AG060726 (N.J.T., and G.C.). Other support includes University of California Davis Flow Cytometry Shared Resource Laboratory with funding from the National Cancer Institute grant P30 CA093373.